

Bose-Einstein condensation in finite drops of α particles

L. M. Satarov,¹ I. N. Mishustin,¹ and H. Stoecker^{1,2,3}

¹*Frankfurt Institute for Advanced Studies,
D-60438 Frankfurt am Main, Germany*

²*Institut für Theoretische Physik, Goethe Universität Frankfurt,
D-60438 Frankfurt am Main, Germany*

³*GSI Helmholtzzentrum für Schwerionenforschung GmbH, D-64291 Darmstadt, Germany*

arXiv:2112.12539v2 [nucl-th] 4 Jul 2022

Abstract

Ground-state properties of finite drops of α particles (Q-balls) are studied within a field-theoretical approach in the mean-field approximation. The strong interaction of α 's is described by the scalar field with a sextic Skyrme-like potential. The radial profiles of scalar- and Coulomb fields are found by solving the coupled system of Klein-Gordon and Poisson equations. The formation of shell-like nuclei, with vanishing density around the center, is predicted at high enough attractive strength of Skyrme potential. The equilibrium values of energy and baryon number of Q-balls and Q-shells are calculated for different sets of interaction parameters. Empirical binding energies of α -conjugate nuclei are reproduced only if the gradient term in the Lagrangian is strongly enhanced. It is demonstrated that this enhancement can be explained by a finite size of α particles.

I. INTRODUCTION

The formation of α -particle clusters and quartic correlations in nuclei are interesting phenomena, that have been in the focus of theoretical and experimental studies for many years, see, e.g., Refs. [1–3]. Several phenomenological and microscopic models have been suggested to describe clustering in nuclei and nuclear matter (see Ref. [4] for a recent review). For example, a relativistic mean-field model with light clusters has been used [5] to calculate their radial profiles in heavy nuclei. It was conjectured that such clusters occupy predominantly the dilute nuclear periphery.

Especially interesting is the possibility of Bose-Einstein condensation (BEC) of α clusters in so-called ' α -conjugate' nuclei, which have even proton and neutron numbers $Z = N = A/2$ (see Ref. [6] and references therein). Earlier we have studied charge-neutral infinite systems of α [7, 8] and $\alpha + N$ [9–11] particles in the mean-field approximation, using Skyrme-like effective interactions. Both the BEC and the liquid-gas phase transition had been considered. The phase diagrams of the α - and $\alpha + N$ matter were found to be qualitatively similar to that observed for liquid ${}^4\text{He}$.

In the present paper we consider finite systems of charged bosons, described by a scalar mean field including also Coulomb interactions. Such a field-theoretical approach was introduced originally in Refs. [12, 13] for so-called Q-ball solitons. The ground states of Q-balls with attractive interactions of bosons were studied in more details by Coleman [14]. Properties of charged Q-balls, with Skyrme-like effective interactions, were considered in Ref. [15].

Q-ball solutions were used to describe heavy α -clustered nuclei in Ref. [16].

One can consider Q-balls as localized, coherent superpositions of bosons similar to atomic Bose condensates in magnetic traps. Properties of such condensates are well described by the Gross-Pitaevskii equation [17, 18]. As demonstrated in Ref. [19], the latter is a non-relativistic analogue of the Klein-Gordon equation for scalar fields of Q-balls. Introducing Q-balls was rather successful in particle physics and astrophysics (see, e.g., Ref. [20]). In particular, gravitating Q-balls are candidates for bosonic stars [21] and dark matter [22]. However, properties of charged Q-balls, and, especially, their stability criteria are still not fully explored. For instance, a new type of soliton solutions, with vanishing scalar density around the center ('Q-shells') have been found recently [23–25] for certain classes of boson self-interactions.

In the present paper we study the ground states (GS) of spherical Q-balls and Q-shells made of charged α particles. The strong interactions of α 's are described by a Skyrme-like scalar potential containing attractive and repulsive terms. First we use interaction parameters determined in Ref. [8] by fitting the microscopic calculations [26] for homogeneous uncharged α matter. Then, the sensitivity of the results to variation of these parameters is analyzed.

We emphasize that α -clustered nuclei, are not necessarily the stable ground states. Some of such nuclei may be metastable excited states, as, e.g., the 3α Hoyle state in ^{12}C at excitation energy 7.65 MeV. Similarly, α -clustered excited states may exist in heavier nuclei, even with charge numbers of up to $Z \sim 80$, as follows from the analysis in Ref. [6]. It was shown within the density functional approach [27] that cluster formation probabilities indeed become larger in excited states of α -conjugate nuclei. As demonstrated in Ref. [28, 29], α -clustered nuclei can be created in heavy-ion reactions at intermediate and relativistic energies. The separation of α -clustered and nucleonic states of nuclear matter can be explained by the existence of a potential barrier between these two phases [11].

The paper is organized as follows: The model Lagrangian is introduced in Sec. IIA, where the equations of motion for the scalar field and electrostatic potential are also derived. In Sec. IIB we show how the particle numbers and binding energies of Q-balls are calculated. In Sec. IIC we discuss a limiting case of homogeneous, uncharged α matter and introduce the constraints on the interaction parameters.

The radial profiles of the baryon density, Coulomb potential and particle effective mass are

calculated in Sec. IIIA and IIIB for both, Q-ball and Q-shell configurations. Their binding energies are analyzed in Sec. IVA for different sets of model parameters. Section IVB demonstrates that empirical binding energies of α -conjugate nuclei can be reproduced only when the gradient term in the effective Lagrangian is significantly enhanced. It is argued that such enhancement can be explained by finite-size effects in the $\alpha\alpha$ interaction. Life times of metastable Q-balls are estimated in Sec. V.

The numerical procedure is explained in Appendix A. The surface tension coefficient of cold α matter is calculated analytically and compared with the corresponding value for isospin-symmetric nuclear matter in Appendix B.

II. CHARGED Q-BALLS IN THE MEAN-FIELD APPROXIMATION

A. Equations of motion for scalar and Coulomb fields

In this paper finite systems of charged, massive bosonic particles are studied by taking into account both strong- and Coulomb interactions. All numerical calculations are performed for finite systems of α particles. Below we apply a field-theoretical approach denoting by $\phi(x)$ and $A^\nu(x)$ the scalar and electromagnetic fields at the space-time point $x^\nu = (t, \mathbf{r})^\nu$. Generally, the Lagrangian density of a bosonic system can be written as [15] ($\hbar = c = 1$):

$$\mathcal{L} = \frac{1}{2} D_\nu \phi (D^\nu \phi)^* - U(|\phi|) + \mathcal{L}_{\text{em}}, \quad (1)$$

where $D_\nu = \partial_\nu - iqA_\nu$ ($q = 2e$ is the charge of the α particle), $U(|\phi|)$ is the mean-field potential, which describes strong self-interactions of α 's, and the last, electromagnetic, term reads

$$\mathcal{L}_{\text{em}} = -\frac{1}{16\pi} F_{\nu\sigma} F^{\nu\sigma}, \quad F_{\nu\sigma} = \partial_\nu A_\sigma - \partial_\sigma A_\nu. \quad (2)$$

Obviously, the Lagrangian (1) is locally gauge-invariant. The corresponding conserved current is

$$J_\nu = \text{Im} (\phi^* D_\nu \phi). \quad (3)$$

In the following only GS of spherical- and nonrotating Q-balls at zero temperature are studied. In this case one can write $\phi = e^{i\mu t} \varphi(r)$ and $A_\nu = A(r) \delta_{\nu,0}$, where φ and A are positive (real) functions, and μ is the chemical potential¹. Then one has $J_\nu = n(r) \delta_{\nu,0}$,

¹ In the literature on Q-balls, it is usually denoted by ω .

where $n = J_0$ is the number density of the α particles:

$$n = (\mu - qA)\varphi^2. \quad (4)$$

The Lagrangian density can be written as

$$\mathcal{L} = \frac{1}{2}(\mu - qA)^2\varphi^2 - \frac{1}{2}(\nabla\varphi)^2 - U(\varphi) + \frac{1}{8\pi}(\nabla A)^2. \quad (5)$$

Variation with respect to φ and A leads to the following coupled equations:

$$\Delta\varphi + (\mu - qA)^2\varphi = U'(\varphi), \quad (6)$$

$$\Delta A + 4\pi qn = 0. \quad (7)$$

Equation (6) can be rewritten in the form of the Klein-Gordon equation (KGE), with the effective mass squared

$$M^2 = U'(\varphi)/\varphi. \quad (8)$$

Equation (7) is the Poisson equation with the charge density qn , where n is defined in Eq. (4). Stable Q-balls are characterized by the following boundary conditions, at small and large r :

$$\varphi'(0) = 0, \quad A'(0) = 0, \quad (9)$$

$$\varphi(r), \quad A(r) \rightarrow 0 \quad \text{at } r \rightarrow \infty. \quad (10)$$

Using Eqs. (6) and (8), one can see that for $\Delta\varphi = 0$ the KGE is satisfied if $\mu - qA = M$. Therefore, the homogeneous solution ($\varphi = \text{const}$) is possible only when

$$\mu = M + qA. \quad (11)$$

This relation may be regarded as a generalization of the well-known BEC condition $\mu = M$ [8], for uncharged bosonic matter. Note that Eq. (11) is gauge-invariant. Our calculations show (see Fig. 2 below) that Eq. (11) holds approximately, for central regions of large Q-balls.

B. Particle number and binding energy of Q-balls

The total number of particles in a Q-ball and its baryon number B are found by integrating the density n over the whole volume:

$$Q = B/4 = 4\pi \int_0^\infty (\mu - qA)\varphi^2 r^2 dr. \quad (12)$$

Note, that in our grand canonical approach, Q is, in general, a noninteger quantity. One should bear in mind that the mean-field approximation, used in this paper, is not justified for small Q-balls, with $Q \lesssim 1$.

From the Lagrangian, the energy-momentum tensor $T_{\nu\sigma}$ of Q-balls as well as profiles of the energy density ε and pressure p can be calculated. One gets (see, for details, Ref. [30])

$$T_{00} = \varepsilon = \varepsilon_k + U + \varepsilon_{\text{gr}} + \varepsilon_c, \quad (13)$$

$$T_{rr} = \varepsilon_k - U + \varepsilon_{\text{gr}} - \varepsilon_c = p + \frac{4}{3}(\varepsilon_{\text{gr}} - \varepsilon_c). \quad (14)$$

Here

$$\varepsilon_k = \frac{1}{2}(\mu - qA)^2\varphi^2, \quad \varepsilon_{\text{gr}} = \frac{1}{2}(\nabla\varphi)^2, \quad \varepsilon_c = \frac{1}{8\pi}(\nabla A)^2 \quad (15)$$

are, respectively, the kinetic, gradient and Coulomb contributions to the energy density.

The total energy E and the binding energy per particle W are obtained by integrating ε over the whole volume:

$$E = (m - W)Q = 4\pi \int_0^\infty \varepsilon r^2 dr, \quad (16)$$

where $m \simeq 3727.3$ MeV is the mass of a single α particle. The binding energy per nucleon equals $W_B = m_N - E/B = (W + B_\alpha)/4$, where $m_N \simeq 938.9$ MeV is the nucleon mass and $B_\alpha = 4m_N - m \simeq 28.3$ MeV is the binding energy of the α particle.

Using Eqs. (6)–(7), (12)–(16), one can prove the validity of the thermodynamic relation [14]

$$dE = \mu dQ, \quad (17)$$

which connects differentials of E and Q at zero temperature. This justifies our interpretation of μ as the chemical potential. The necessary conditions for the Q-ball stability can be written as

$$\Delta \equiv m - \mu > 0, \quad W > 0. \quad (18)$$

The first inequality implies that the escape of a single α particle from the Q-ball's surface to infinity is energetically forbidden [15]². The calculations show that the conditions (18) are fulfilled in the interval $Q_{\text{min}} < Q < Q_{\text{max}}$ where Q_{min} and Q_{max} correspond, respectively, to $W = 0$ and $\Delta = 0$.

² As discussed in Appendix A, the region $\mu > m$ corresponds to continuum states, with φ oscillating at $r \rightarrow \infty$. However, these states are, in fact, metastable, due to presence of the Coulomb barrier.

Following Refs. [8, 16], the mean-field potential $U(\varphi)$ is parameterized in the Skyrme-like form

$$U(\varphi) = \frac{m^2}{2}\varphi^2 - \frac{a}{4}\varphi^4 + \frac{b}{6}\varphi^6, \quad (19)$$

where a and b are positive parameters, which determine, respectively, the attractive and repulsive interactions of α particles. Similar self-interactions of scalar bosons have been considered in Refs. [15, 30, 31]. The above expression can be rewritten as

$$\frac{U}{\varphi^2} = \frac{b}{6}(\varphi^2 - \varphi_0^2)^2 + \frac{m^2}{2}\left(1 - \frac{1}{\Lambda}\right). \quad (20)$$

Here

$$\varphi_0 = \sqrt{\frac{3a}{4b}}, \quad \Lambda = \frac{16bm^2}{3a^2} \quad (21)$$

are the parameters which determine the main characteristics of the Q-balls, as well as properties of equilibrium, uncharged α matter (see detailed calculations in Ref. [8]). In particular, φ_0^2 is the equilibrium scalar density of a homogeneous Bose-Einstein condensate at zero temperature.

Substituting (19) into Eq. (8) gives the equation for the effective mass squared

$$M^2 = m^2 - a\varphi^2 + b\varphi^4. \quad (22)$$

One can see that $M^2(\varphi_0) = m^2(1 - \Lambda^{-1})$ is nonnegative at $\Lambda \geq 1$ ³.

C. Properties of homogeneous, uncharged α matter

If the Coulomb field is switched off ($q \rightarrow 0$), Q-balls could be arbitrary large. At zero temperature such hypothetical, 'uncharged' α matter has the GS characterized by a spatially homogeneous scalar field, $\varphi = \varphi_0$. This value corresponds to the minimum of $U(\varphi)/\varphi^2$ [14]. Indeed, applying formulas of preceding section for a homogeneous, uncharged system with $\nabla\varphi = 0, A = 0$, one gets the following relations

$$\frac{\varepsilon}{n} = \frac{\mu}{2} + \frac{U(\varphi)}{\mu\varphi^2}, \quad \mu = M(\varphi). \quad (23)$$

Therefore, the minimum of the energy per particle ε/n is found by minimizing U/φ^2 . The second condition in Eq. (23) is obtained from the KGE for homogeneous uncharged matter

³ As pointed out in Ref. [32], the bosonic vacuum becomes unstable at $\Lambda < 1$. This does not occur for the Skyrme parameters expected for α interactions.

(see Eqs. (6) and (8)). It is interesting that it coincides with the generalized condition of Bose-Einstein condensation as introduced in Ref. [8]. By using Eqs. (23) one obtains the following characteristics of the α -matter GS

$$\mu = \min\left(\frac{\varepsilon}{n}\right) = m\sqrt{1 - \frac{1}{\Lambda}}. \quad (24)$$

Adjusting the binding energy $W = m - \mu$ and the density $n = \mu\varphi_0^2$ to the GS properties of homogeneous uncharged α matter, as obtained by microscopic calculations in Ref. [26], we extracted the values (for details, see Ref. [8])

$$a = 7853, \quad b = 78.94 \text{ MeV}^{-2}. \quad (25)$$

Below this parameter choice is denoted as Set I.

There exists an additional constraint on Λ [7], which follows from the obvious condition, namely, that α matter has to be less bound than isospin-symmetric nuclear matter in the GS. It is commonly accepted that such matter has the binding energy per baryon $W_{\text{SM}} \simeq 16 \text{ MeV}$. On the other hand, in accordance with Eq. (24), in the limit of large Λ the binding energy of α matter per particle equals $W \simeq m/(2\Lambda)$. Therefore, one gets the condition

$$W_B \simeq \frac{1}{4} \left(\frac{m}{2\Lambda} + B_\alpha \right) < W_{\text{SM}}. \quad (26)$$

This is equivalent to $\Lambda > 52$ (approximately) or

$$\frac{a}{\sqrt{b}} < 1190 \text{ MeV}. \quad (27)$$

For $b \sim 80 \text{ MeV}^{-2}$ (which is close to the value assumed in Set I) one obtains the constraint⁴ $a \lesssim 1.1 \cdot 10^4$.

III. GROUND-STATE PROPERTIES OF CHARGED Q-BALLS.

A. Radial profiles of density and effective mass

Using the effective potential (19) we have solved numerically coupled equations (6) and (7) for different values of interaction parameters a and b . Similar calculations have been done

⁴ Note that the parameters $b = 30.73 \text{ MeV}^{-2}$ and $a = 3 \cdot 10^4$ used in Ref. [16] violate the constraint (27), which results in an unrealistically large binding energy of α matter $W_B \simeq 214 \text{ MeV}$.

earlier in Refs. [15, 30, 31]. It was shown that, in general, for a given μ there exist two stable Q-ball configurations with different effective radii, energies and particle numbers. However, the previous authors did not analyze in detail the sensitivity to the model parameters and did not specify bosonic particles bound in Q-balls. We also make comparison with empirical data [6, 33] on α -conjugate nuclei. Characteristics of stable Q-balls, calculated for the

TABLE I. Characteristics of Q-balls for different values of chemical potential $\mu = m - \Delta$ calculated for parameter Set I.

Δ , MeV	Q	W , MeV	$\varphi(0)/\varphi_0$	$qA(0)$, MeV
0 ^a	14.1	5.6	0.896	25.5
2	11.8	6.6	0.924	22.4
4	9.0	7.6	0.949	19.2
6	6.7	8.6	0.971	15.9
8	4.5	9.3	0.994	12.3
10	2.4	9.6	1.022	8.0
10.7	1.2	8.8	1.042	5.0
10.1	0.52	6.5	1.057	2.8
9.1	0.32	4.4	1.054	1.9
5.5	0.14	0.01	0.958	0.9

^a The results for $\Delta = 0$ are obtained by setting $\Delta = 10^{-4}$ MeV.

parameter Set I (see Eq. (25)) are shown in Table I. The last two columns give the central values of the scalar- and Coulomb fields. Note that $\varphi(0) \simeq \varphi_0$ where φ_0 is given by Eq. (21) which implies a rather good accuracy of the 'thin wall' approximation [15], even for $Q \sim 1$. According to Table I, the maximum particle number for stable states $Q_{\max} \simeq 14$ corresponds to $\Delta = 0$ (i.e. $\mu = m$). However, due to the presence of the Coulomb barrier we expect the formation of metastable Q-balls even for $\Delta < 0$ (see Sec. V).

Figures 1 and 2 show the profiles of the baryon density, Coulomb potential and effective mass for different μ . One can see a central density suppression, especially well visible for $\Delta \lesssim 5$ MeV. This effect is due to the repulsive Coulomb interaction, and it does not appear for uncharged Q-balls (see, e.g., Ref. [15]). A similar central depletion of proton density was predicted in the relativistic mean-field model of Ref. [34] for superheavy nuclei with $Z \sim 120$. According to Fig. 2, in the case $\mu = m$, the Q-ball's chemical potential is, in fact, the result of cancellation between the attractive well of the depth $m - M$ and the

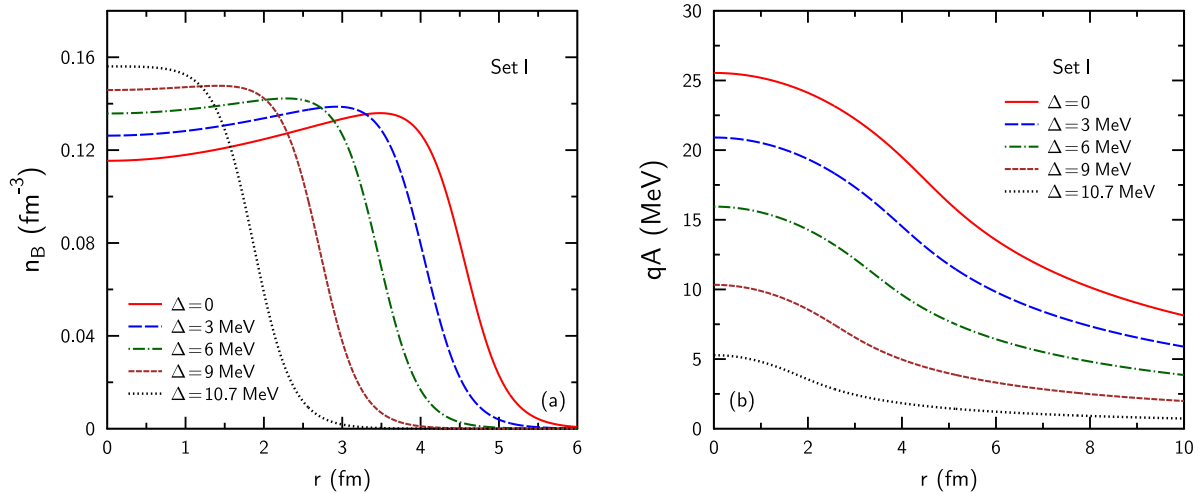


FIG. 1. Radial profiles of the baryon density $n_B = 4n$ (a) and Coulomb potential qA (b) for different values of the chemical potential $\mu = m - \Delta$, calculated for the parameter Set I.

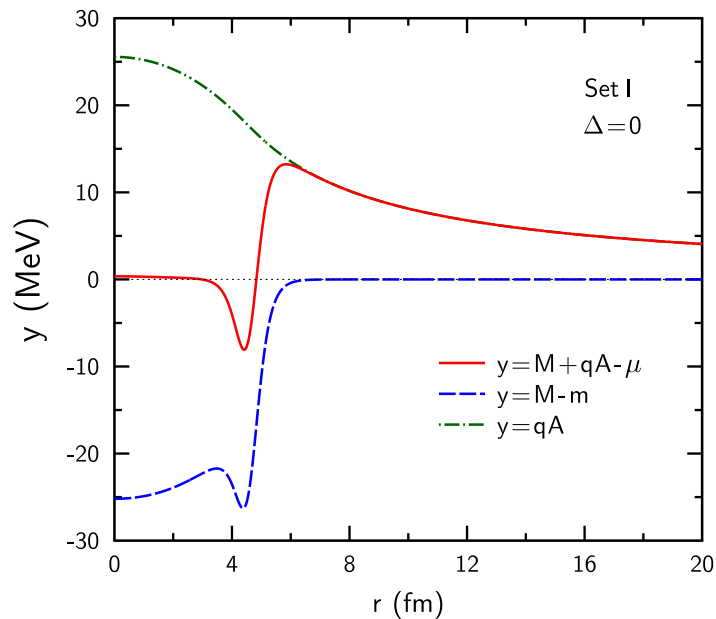


FIG. 2. The radial profiles of $M + qA - \mu$ (the solid line), $M - m$ (the dashed curve) and qA (the dash-dotted line), for $\Delta = m - \mu = 0$ and the parameter Set I.

repulsive Coulomb energy qA at $r < R \simeq 5 \text{ fm}$ ⁵. This cancellation does not occur at larger

⁵ Note that for $\Delta = 0$ the central electrostatic potential $qA(0)$ is close to the value $3q^2Q/(2R) \simeq 24 \text{ MeV}$ for a homogeneously charged sphere with the radius R and total charge Q . One can also see that the height of the Coulomb barrier at $r = R$ is approximately equal to $q^2Q/R \simeq 16 \text{ MeV}$.

radii, where the nuclear potential disappears and the Coulomb barrier dominates.

B. Two types of solutions: Q-balls and Q-shells

We have investigated possible solutions of field equations for different sets of model parameters. It was found that a new class of solutions appears for large enough values of the attraction coefficient a . Namely, the model predicts the formation of hollow, shell-like structures with vanishing baryon density in the central region. To distinguish these two types of solutions, we call them Q-balls and Q-shells, respectively. The appearance of Q-shells was demonstrated in Refs. [23–25].

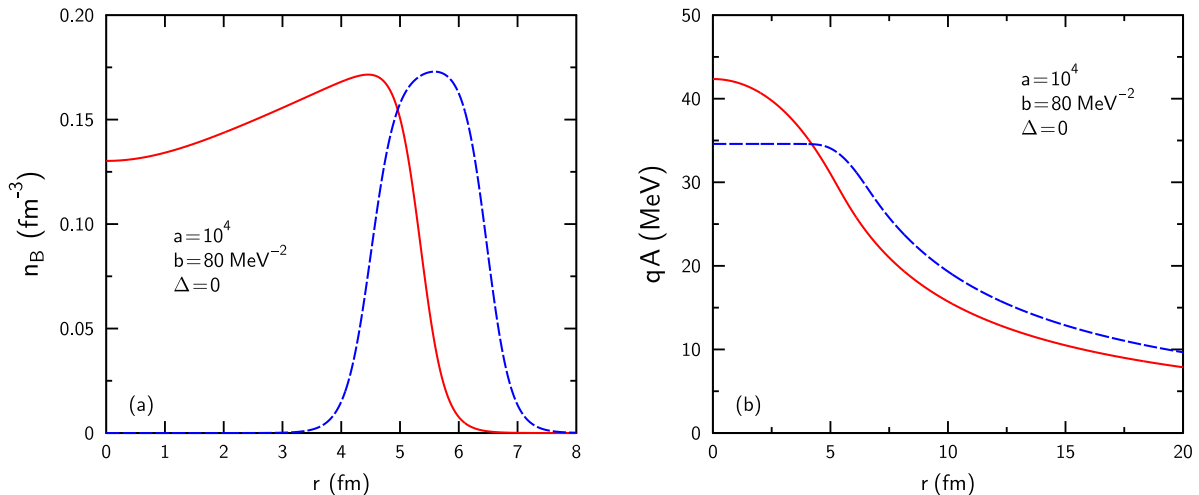


FIG. 3. The profiles of baryon density (a) and Coulomb potential (b) for $\mu = m$ and the parameters $a = 10^4$, $b = 80 \text{ MeV}^{-2}$. Solid and dashed lines correspond to the Q-ball and Q-shell solutions, respectively.

The calculations show that stable Q-shells do not exist for the parameter Set I. According to our analysis, at $b \simeq 80 \text{ MeV}^{-2}$ they appear only for $a \gtrsim 9 \cdot 10^3$ and small enough Δ values. Figure 3 represents the radial profiles of the baryon density and Coulomb potential, as obtained for $a = 10^4$, $b = 80 \text{ MeV}^{-2}$ and $\Delta = 0$. These parameters yield the values $Q \simeq 27.3$, $W \simeq 10.1 \text{ MeV}$ for the Q-ball solution, while $Q \simeq 33.5$, $W \simeq 8.5 \text{ MeV}$ for the Q-shell. The new shell-like solution corresponds to larger (smaller) values of gradient (Coulomb) energy per particle.

Figure 4 shows the results for the same parameters a, b , but for nonzero Δ value, cor-

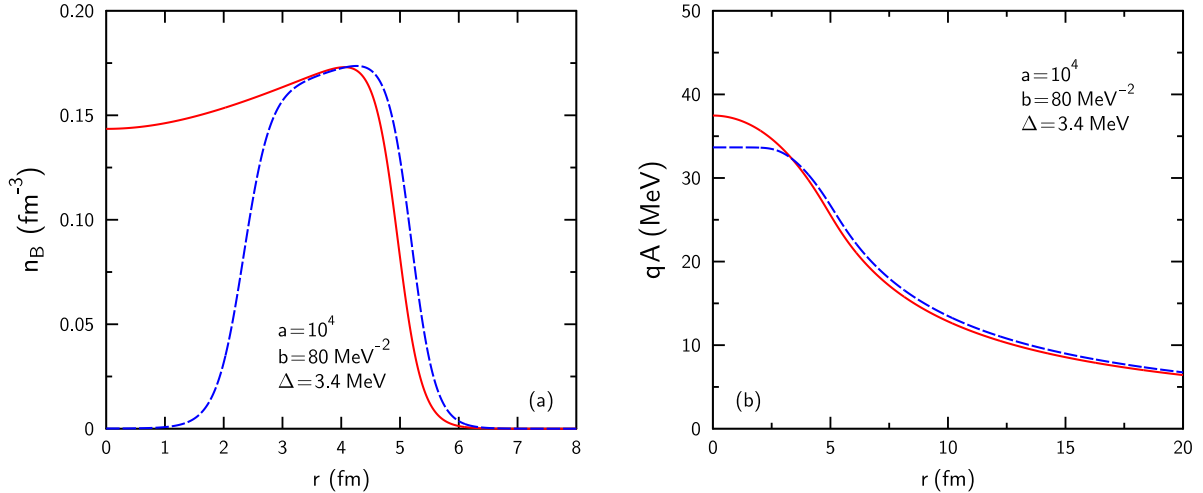


FIG. 4. Same as Fig. 3, but for $\Delta = 3.4$ MeV.

responding to smaller μ . Reducing the chemical potential gives rise to shifting the outer surface of a Q-shell towards the Q-ball's surface. This is seen in Fig. 4 where Q-ball and Q-shell profiles are considered for $\Delta = 3.4$ MeV⁶. In this case the model predicts closer characteristics: $Q \simeq 23.4, W \simeq 11.5$ MeV and $Q \simeq 22.3, W \simeq 11.0$ MeV, for the Q-ball and Q-shell configurations, respectively. These two configurations with close values of Q may be regarded as density isomers, separated by a potential barrier.

The sensitivity of Q-shell properties to the model parameters will be considered in the next section.

IV. SYSTEMATICS OF BINDING ENERGIES OF Q-BALLS AND Q-SHELLS

A. Comparison with empirical binding energies of α -conjugate nuclei

In this section we consider how the present model is able to reproduce the 'experimental' data. The GS binding energies of α -conjugate nuclei (with $Z = N = 2Q$) were compiled by von Oertzen in Ref. [33]. It was conjectured that such nuclei can be regarded as made of α particles. The compiled data are shown below by dots.

Figure 5 shows the Q-ball binding energy W as a function of Q for the parameter Set I. The right end point of the $W(Q)$ curve, corresponding to the chemical potential $\mu = m$, gives

⁶ At larger values of Δ , Q-shell solutions disappear for the values of interaction parameters considered here.

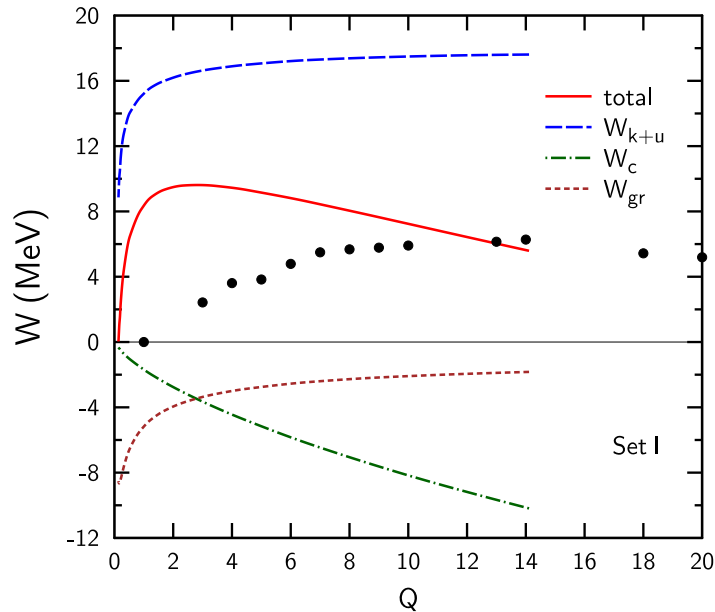


FIG. 5. Binding energy per particle, W , as a function of the total number of α 's, Q , for parameter Set I (the solid line). The combined contribution of the kinetic and potential parts of the Q-ball's energy is shown by the long-dashed curve. The Coulomb and gradient energies are shown by the dash-dotted and short-dashed lines, respectively. Dots are empirical values of the binding energies of α -conjugate nuclei with $A = 4Q$ from Ref. [33].

the maximal possible number of α particles in a stable Q-ball. At $\mu > m$, Q-balls become metastable, as it is energetically possible for α 's to leave the system and go to infinity. However, at not too large $\mu - m$, this process is strongly suppressed by the Coulomb barrier (see Fig. 2). The life times of these metastable states can be very long as known from α -decays of ordinary nuclei, see Sec. V. Therefore, the region $\mu > m$ is also included in our analysis.

In Fig. 5 we show separately different contributions to the Q-ball's energy per particle. They were calculated by using the corresponding energy density terms in Eq. (15). Note, that the absolute value of the gradient energy per particle decreases, while the Coulomb contribution increases with Q . Obviously, our mean-field approach is not reliable at $Q \lesssim 1$.

One can see, that the model predictions with the parameter Set I strongly deviate from the empirical data. In particular, binding energies of lighter nuclei, with $Q \lesssim 10$, are significantly overestimated. In principle, one can find such model parameters a and b which

allow a good fit for any individual α -conjugate nucleus, as, e.g., ^{52}Fe ($Q = 13$) in Fig. 5, but then it is not possible to fit the empirical data for other α -conjugate nuclei in the whole mass-number interval. Nevertheless, the shape of the binding energy curve is qualitatively similar to that predicted by Weizsäcker's formula [35] for ordinary nuclei. Namely, binding energies drop at small Q due to the surface energy, and at large Q because of the Coulomb repulsion.

Figure 6 demonstrates the sensitivity of binding energies $W(Q)$ to the choice of the interaction parameters a and b . Again one can see that the model predictions are in strong disagreement with empirical data, and it is not possible to improve the fit just by choosing parameters significantly different from Set I.

By analyzing these results one can make the following conclusions: first, the boundaries of the Q-ball and Q-shell stability ($\Delta = 0$) shift to larger Q-values with increasing a or decreasing b ⁷. Second, Q-shells appear only at large enough Q , and threshold Q-values where they become more bound as compared to Q-balls (see crosses in Fig. 6) increase (decrease) with a (b). Note, that in the case of the parameter Set I this threshold shifts to the region of the Q-ball metastability, i.e, outside the end points of the dash-dotted lines in Fig. 6.

Inspecting Figs. 5 and 6 suggests that the large deviation from the data is caused by too small surface energy, which is generated by the gradient term (GT) ε_{gr} (see Eq. (15)). Indeed, as shown in the next section, agreement with the empirical data can be achieved by a significant enhancement of the GT.

B. Modification of the gradient term

A simple analysis shows that the predicted surface tension of cold α matter, is unrealistically small, of the order of $0.2 \text{ MeV}/\text{fm}^2$ for the parameter Set I (see Appendix B). This is by a factor of 5 smaller than the empirical value for ordinary nuclei. To avoid this drawback, we have modified the GT of Lagrangian (5) by the replacement $(\nabla\varphi)^2 \rightarrow \xi_s(\nabla\varphi)^2$ where $\xi_s \geq 1$ is the enhancement factor. This leads to the appearance of additional coefficient ξ_s in front of the Laplacian in the KGE (6). The same factor also appears in the gradient part of the energy density ε_{gr} . Our calculations show (see Figs. 7 and 8) that this modification

⁷ As shown in Appendix B this leads to increased values of the surface tension.

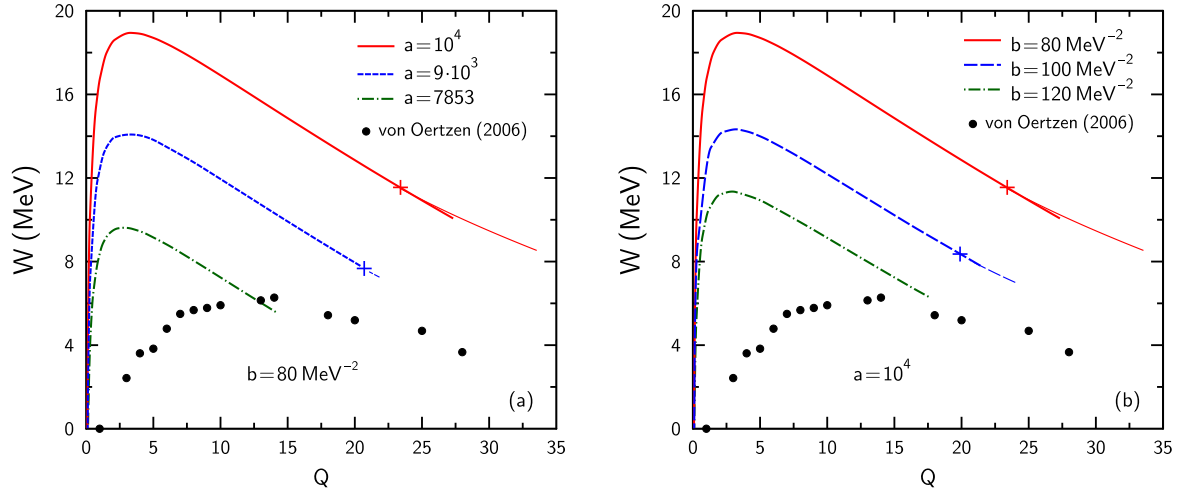


FIG. 6. Binding energies per particle as functions of particle number Q for different values of the parameters a and b , shown in the left and right panels. Thick and thin lines correspond to Q-balls and Q-shells, respectively. Crosses mark left boundaries of domains where stable Q-shells exist. Dots are empirical data extracted [33] from observed masses of α -conjugate nuclei.

of the model leads to smoothing density profiles and reducing binding energies for Q-balls with $Q \lesssim 15$.

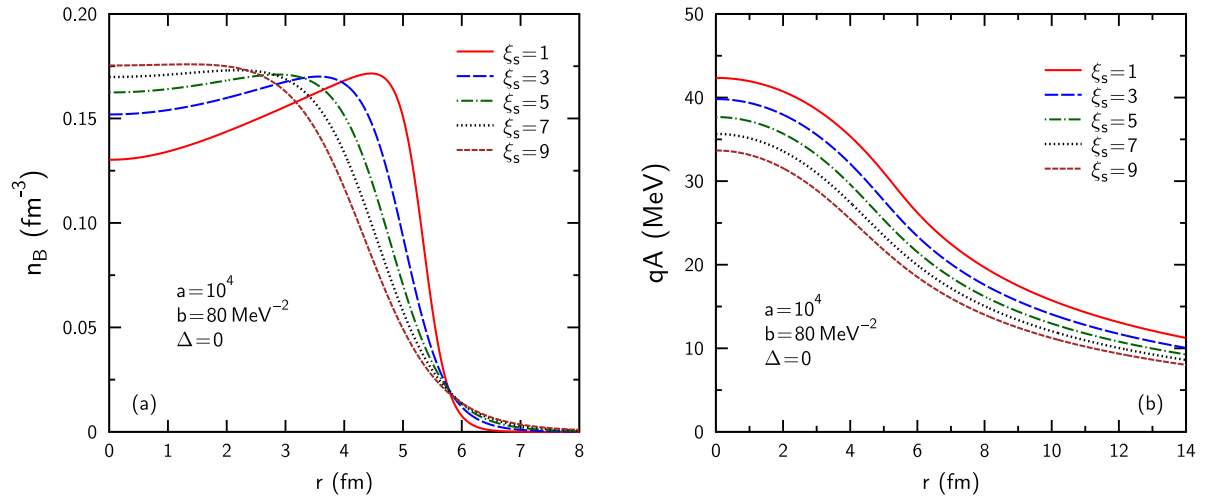


FIG. 7. Profiles of the baryon density (a) and Coulomb potential (b) for different values of the gradient enhancement factor ξ_s .

Figure 8 shows that the empirical data can be well reproduced with large $\xi_s \sim 8 - 9$.

As shown in Appendix B, the resulting surface tension coefficient becomes similar to that

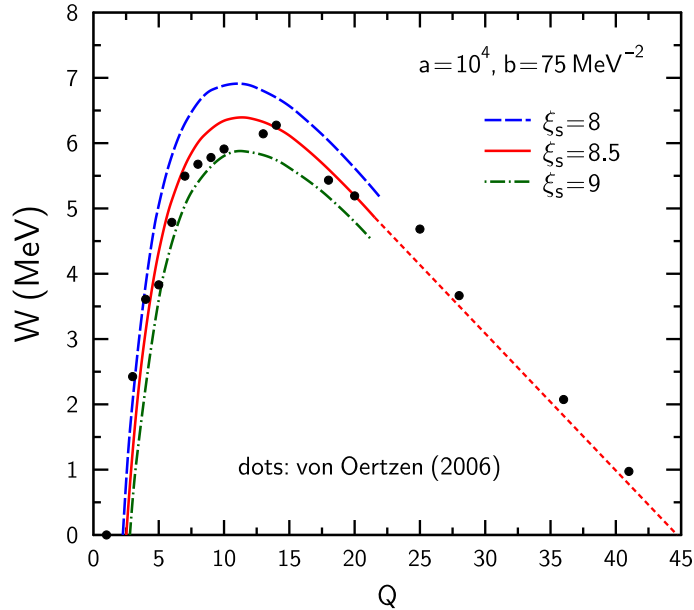


FIG. 8. Binding energy W as the function of Q for $a = 10^4$, $b = 75 \text{ MeV}^{-2}$ and $\xi_s = 8, 8.5$ and 9 . Short-dashed line is obtained by linear extrapolation of the solid curve to the region $Q > Q_{\max}$ where $Q_{\max} \simeq 21.5$ is the particle number corresponding to $\mu = m$ for $\xi_s = 8.5$.

for ordinary nuclei. In Fig. 8 the results for $\xi_s = 8.5$ are extrapolated into the region of metastable nuclei with $Q > Q_{\max}$ (the short-dashed line). Note that the extrapolation is close to the empirical data even at large Q . From this analysis we conclude that these data can be well described by the model parameters $a = 10^4$, $b = 75 \text{ MeV}^{-2}$ and $\xi_s = 8.5$ (Set II).

C. Importance of finite-size effects

Of course, such a strong modification of the GT needs to be explained. From the density profiles in Fig. 7 one can see that at $\xi_s \lesssim 3$, surface widths of Q-balls are smaller than the rms radius of α particle $R_\alpha \simeq 1.7 \text{ fm}$ [36]. This unrealistic behavior follows from the point-like character of strong interaction assumed in the Skyrme potential (19). In reality, α particles are extended objects which can be described by a (normalized) Gaussian density distribution

$$F(r) = \frac{\lambda^3}{\pi^{3/2}} \exp(-\lambda^2 r^2), \quad (28)$$

where the parameter $\lambda \sim R_\alpha^{-1}$. Therefore, the attractive interaction of α particles is only possible at distances $\Delta r \gtrsim 2R_\alpha$ ⁸.

One can estimate this finite-size effect by adding the correction term to the Lagrangian⁹

$$\delta\mathcal{L} = \frac{a}{4} \int F(R) \left[\varphi^2 \left(\mathbf{r} + \frac{\mathbf{R}}{2} \right) \varphi^2 \left(\mathbf{r} - \frac{\mathbf{R}}{2} \right) - \varphi^4(\mathbf{r}) \right] d^3R, \quad (29)$$

where R is the distance between the α -particle centers. Expanding the expression in square brackets up to the lowest order in R and neglecting the curvature terms, we obtain

$$\delta\mathcal{L} \simeq -\frac{a}{24} \varphi^2(\mathbf{r}) (\nabla\varphi)^2 \int F(R) R^2 d^3R. \quad (30)$$

After adding $\delta\mathcal{L}$ to the Lagrangian (5) one can see that the GT is enhanced by the factor

$$\xi_s \simeq 1 + \frac{a}{8\lambda^2} \varphi^2(\mathbf{r}) \sim 1 + \frac{k_0^2}{4\lambda^2}. \quad (31)$$

Here we have taken $\varphi^2 \sim \varphi_0^2/2$, where φ_0 is defined in Eq. (21), and introduced the characteristic momentum k_0 from Eq. (A2). For the parameter set with $a = 10^4$, $b = 75 \text{ MeV}^{-2}$, one has $k_0 = 2.53 \text{ fm}^{-1}$. Substituting $\lambda = 0.5 \text{ fm}^{-1}$ we obtain the enhancement factor $\xi_s \sim 7.4$ which is close to the value extracted from the fit of data on α -conjugate nuclei (see Fig. 8).

V. ESTIMATING LIFE TIMES OF METASTABLE Q-BALLS

Life times of metastable Q-balls can be estimated by using standard formalism for α -decay of ordinary nuclei [37, 38]. We approximate the α -particle potential in the Q-ball by a combination of an attractive square well with radius R and the repulsive Coulomb barrier $V(r) = q^2Q/r$ at $r > R$, where Q is total number of α particles in the Q-ball. One can estimate the single-particle (nonrelativistic) energy of α 's in a metastable state as

$$E \simeq \mu - m \simeq \frac{3q^2}{2R} (Q - Q_m) > 0, \quad (32)$$

where Q_m is the maximal value of Q for stable states. We neglect the energy spreading due to a nonzero decay width. It is also assumed that μ changes linearly with the Coulomb potential at $r = 0$ (see footnote on page 10). In the following we neglect the Q -dependence

⁸ At smaller distances, a repulsive interaction of the van der Waals type should be also included.

⁹ In the limit of a point-like interaction ($\lambda \rightarrow \infty$) one has $F(R) \rightarrow \delta(\mathbf{R})$ and $\delta\mathcal{L} \rightarrow 0$.

of R estimating it by the value at $Q = Q_m$. The condition $0 < E < V(R)$ is fulfilled if $Q_m < Q < 3Q_m$.

In the semiclassical approximation, the probability of α particle with the energy E to penetrate the Coulomb barrier is

$$P(E) = \exp \left\{ -\frac{2}{\hbar} \int_R^{r_{\max}} \sqrt{2m [V(r) - E]} dr \right\}, \quad (33)$$

where $r = r_{\max}$ is determined from the equation $V(r) = E$. The integral in Eq. (33) can be

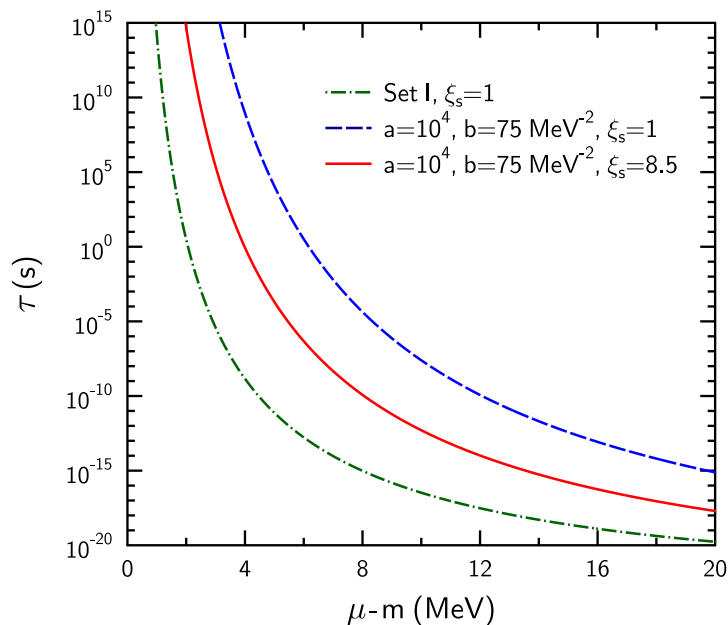


FIG. 9. Lifetimes of metastable Q-balls at $\mu > m$ for different sets of model parameters.

calculated analytically that gives

$$|\ln P| = \frac{2mv}{\hbar R} I(\alpha), \quad \alpha = \frac{2}{3} \frac{Q}{Q - Q_m}, \quad (34)$$

where $v = \sqrt{2E/m}$ is the mean velocity of α particles at $r < R$ and

$$I(\alpha) = \int_1^\alpha \sqrt{\frac{\alpha}{x} - 1} dx = \alpha \tan^{-1} \sqrt{\alpha - 1} - \sqrt{\alpha - 1}. \quad (35)$$

The life time of the metastable state with energy E can be estimated as

$$\tau(E) \simeq \frac{2R}{vP(E)}. \quad (36)$$

The results of calculating τ as a function of μ is shown in Fig. 9 for different sets of model parameters. Obviously, Q-balls closer to the threshold $\mu = m$ have longer life times, and $\tau \rightarrow \infty$ at $\mu \rightarrow m$. With the 'best fit' parameters corresponding to the solid line in Fig. 9, we predict life times $\tau \gtrsim 10^{-10}$ s for $\mu - m \lesssim 8$ MeV. This is much longer than typical time scales in ordinary nuclei. Such metastable Q-balls emitting multiple α particles could be good candidates for α -clustered nuclei.

VI. CONCLUSIONS

In the present paper we have formulated the mean-field model for describing finite-size systems of charged scalar bosons with Skyrme-like effective interactions. This model is used to study the Bose-Einstein condensation of α particles in drops of nuclear size containing up to 50 α clusters. The baryon density, energy density, and effective mass profiles were calculated for different values of the chemical potential μ . Two types of solutions have been found: Q-balls with nonzero density at the center and Q-shells with vanishing density in the central region. It is shown that stable Q-shells appear only for large enough strengths of attractive interaction.

We have calculated the GS binding energies of Q-balls (Q-shells) as functions of μ and investigated their stability regions. Both stable (with $\mu < m$, where m is the α -particle mass) and metastable ($\mu > m$) solutions were considered. It was shown that life times of metastable Q-balls may be rather long in nuclear scale. Such Q-balls are especially interesting due to the possibility of simultaneous emission of several α particles. These decay channels could be a unique signature of α clustering in nuclei.

We have tried to find the set of model parameters which would fit the empirical binding energies of α -conjugate nuclei compiled in Ref. [33]. It turned out that the standard version of the model with point-like α particles strongly overestimates binding energies of lighter Q-balls. The agreement with empirical data has been achieved only when the gradient term of the Lagrangian was significantly enhanced. It is demonstrated that this enhancement can be naturally explained by a finite size of α 's. We would like to note, that our assumption that ground states of α -conjugate nuclei contain only α particles and no nucleons is probably oversimplified. In the future we are going to study more complicated finite-size alpha-nucleon systems.

ACKNOWLEDGMENTS

The authors thank M. Gorenstein, S. Misicu, and O. Savchuk for useful discussions. L.M.S., and I.N.M. appreciates the support from the Frankfurt Institute for Advanced Studies. H.St. thanks the support from Walter Greiner Gesellschaft zur Förderung der physikalischen Grundlagen e.V. through the J. M. Eisenberg Laureatus chair at Goethe Universität Frankfurt am Main.

APPENDIX A: NUMERICAL PROCEDURE

In this section we describe our numerical procedure for calculating properties of (meta)stable Q-balls (and/or Q-shells). For such calculations it is important to impose suitable asymptotic conditions at large r . At $r \rightarrow \infty$ one can write approximately $U \simeq (m\varphi)^2/2$, and $A \simeq qQ/r$, where Q is the total number of α particles bound in the Q-ball. Then using Eq. (6), one finds following asymptotic behaviour (see for details Ref. [39])

$$\varphi \simeq \text{const} \frac{e^{-\sqrt{m^2 - \mu^2}r}}{r^{1+\beta Q}}, \quad \beta = \frac{q^2 \mu}{\sqrt{m^2 - \mu^2}} \quad (\text{at } r \rightarrow \infty). \quad (\text{A1})$$

One can see that at $\mu > m$ the scalar field becomes a complex function which results in a finite flux at $r \rightarrow \infty$. However, at not too large $\mu - m$ one can consider such systems as metastable nuclei emitting α 's from their surface. Due to presence of the Coulomb barrier, corresponding decay times may be rather long, as demonstrated in Sec. V.

It is useful to define a new function $Q_*(r)$ which is equal to the number of particles within a sphere of radius r (note that $Q_*(0) = 0$ and $Q_* \rightarrow Q$ at $r \rightarrow \infty$). According to the Gauss law of electrostatics, $A'(r) = -qQ_*(r)/r^2$. One can rewrite Eqs. (6)–(7) by introducing the dimensionless quantities $\rho = k_0 r$, $f = \varphi/\varphi_0$, $g = (\mu - qA)/k_0$, where

$$k_0 = \sqrt{m^2 - \mu_0^2} = \frac{m}{\sqrt{\Lambda}}, \quad (\text{A2})$$

is the characteristic momentum scale of the equilibrium α matter¹⁰. We arrive at the fol-

¹⁰ Here we denote its chemical potential as μ_0 and apply Eq. (24) in the second equality.

lowing set of differential equations which determine the profiles of f , g , and Q_*

$$\frac{d^2 f}{d\rho^2} + \frac{2}{\rho} \frac{df}{d\rho} = f (\Lambda - g^2 - 4f^2 + 3f^4), \quad (\text{A3})$$

$$\frac{dg}{d\rho} = \frac{q^2 Q_*}{\rho^2}, \quad (\text{A4})$$

$$\frac{dQ_*}{d\rho} = \frac{16\pi}{a} g (f\rho)^2. \quad (\text{A5})$$

By introducing a spatial grid $\rho_i = hi$, $i = 0, 1, \dots, i_{\max}$, where $h \sim 10^{-2}$ and $i_{\max} \sim 5 \cdot 10^3$, we approximated Eqs. (A3)–(A5) by an algebraic system of finite-difference equations. It was solved by iterations, using the program package 'dsolve' from Numerical Recipes [40]. The initial profiles of $f(\rho)$ and $g(\rho)$ were chosen by using semi-analytic approximations, suggested in Refs. [25, 31].

APPENDIX B: SURFACE TENSION OF Q-BALLS

In this section we analyze the surface tension σ_s of large Q-balls neglecting Coulomb field in the KGE (6). In fact, we derive the surface tension of a cold condensate of (uncharged) bosons interacting with the Skyrme potential (19). We calculate σ_s as follows

$$\sigma_s = (4\pi R^2)^{-1} \int \varepsilon_{\text{gr}} d^3 r \simeq \int_0^\infty \left(\frac{d\varphi}{dz} \right)^2 dz, \quad (\text{B1})$$

where ε_{gr} is defined in Eq. (15). In the second equality, instead of a spherical Q-ball with radius R , a one-dimensional symmetrical slab $-\infty < z < +\infty$ is considered. Such an approximation is justified for large Q . In this case the scalar field $\varphi(z)$ obeys the one-dimensional KGE

$$\frac{d^2 \varphi}{dz^2} + \mu^2 \varphi = \frac{dU}{d\varphi}. \quad (\text{B2})$$

The first integral of this equation is easily obtained

$$\frac{1}{2} \left(\frac{d\varphi}{dz} \right)^2 = U(\varphi) - \frac{\mu^2 \varphi^2}{2} \equiv \Omega(\varphi). \quad (\text{B3})$$

Here we have taken into account that $\varphi, d\varphi/dz \rightarrow 0$ at $|z| \rightarrow \infty$. In fact, this equation implies that pressure $p = T_{zz} = 0$ for all z . In the last equality of (B3) we introduce the thermodynamic potential $\Omega = \varepsilon - \mu n$ for a homogeneous scalar field φ (see Sec. II C). It is easy to see that at the central plane, $z = 0$, one has $d\varphi/dz = 0$ and $\varphi = \varphi_*$, where φ_* is found from the equation $\Omega(\varphi_*) = 0$.

Finally one obtains the relation (first derived in Ref. [14])

$$\sigma_s = \int_0^{\varphi_*} \sqrt{2\Omega(\varphi)} d\varphi. \quad (\text{B4})$$

In the case of Skyrme interaction, substituting (19), one has

$$\sigma_s = k_0 \varphi_0^2 \int_0^{f_*} \sqrt{\eta^2 - 2f^2 + f^4} f df, \quad (\text{B5})$$

where

$$f_* = \sqrt{1 - \sqrt{1 - \eta^2}}, \quad \eta = \frac{1}{k_0} \sqrt{m^2 - \mu^2}. \quad (\text{B6})$$

Here we use the constants φ_0, k_0 defined in Eqs. (21), (A2).

The integral in Eq. (B5) can be calculated analytically. One gets

$$\sigma_s = \sigma_0 F(\eta), \quad (\text{B7})$$

where

$$\sigma_0 = \frac{k_0 \varphi_0^2}{4} = a^2 \left(\frac{3}{16b} \right)^{3/2}, \quad (\text{B8})$$

and

$$F(\eta) = \eta - (1 - \eta^2) \ln \sqrt{\frac{1 + \eta}{1 - \eta}} \quad (\text{B9})$$

is a dimensionless function which monotonically increases from zero to unity in the interval $0 < \eta < 1$. Equations (B7)–(B9) give the analytic expression for σ_s as a function of chemical potential. It is interesting to note that heaviest stable Q-balls with $\mu = m$ have vanishing surface tension. One can see that σ_s reaches its maximal value σ_0 for equilibrium bosonic matter with $\mu = \mu_0$.

Numerical estimates give rather small values for σ_0 . For example, by choosing the parameters a, b from Set I, one obtains $\sigma_0 \simeq 0.18 \text{ MeV/fm}^2$. A somewhat larger value, $\sigma_0 \simeq 0.32 \text{ MeV/fm}^2$, is obtained for $a = 10^4, b = 75 \text{ MeV}^{-2}$. On the other hand, much higher surface tension coefficients are expected for cold ordinary nuclei. Indeed, according to the Weizsäcker mass formula, the nuclear surface energy equals $E_S = a_S A^{2/3}$ where A is the baryon number of the nucleus and $a_S \simeq 17.2 \text{ MeV}$ [41]. Dividing this energy by $4\pi R^2$ (here $R = r_0 A^{1/3} \simeq 1.2 A^{1/3} \text{ fm}$ is the geometrical radius of the nucleus), one obtains the nuclear surface tension coefficient

$$\sigma_{sN} \simeq \frac{a_S}{4\pi r_0^2} \simeq 0.95 \text{ MeV/fm}^2. \quad (\text{B10})$$

This exceeds the value of σ_s predicted for Q-balls by about a factor of three.

Such a discrepancy can be removed by modifying the Laplacian term in the KGE. One can see that introducing the enhancement factor ξ_s in front of Laplacian in Eq. (6) leads to the additional coefficient $\sqrt{\xi_s}$ in the right hand sides of Eqs. (B4) and (B8). Using the value $\xi_s \simeq 8.5$, which enables a good agreement with von Oertzen data (see Fig. 8), we get the estimate $\sigma_0 \simeq 0.94 \text{ MeV/fm}^2$, very close to that obtained in Eq. (B10).

-
- [1] Y. Funaki, H. Horiuchi, W. von Oertzen, G. Röpke, P. Schuck, A. Tohsaki, and T. Yamada, *Phys. Rev. C* **80**, 064326 (2009).
 - [2] T. Sogo, G. Röpke, and P. Schuck, *Phys. Rev. C* **81**, 064310 (2010).
 - [3] J.-P. Ebran, E. Khan, T. Niksic, and D. Vretenar, *Phys. Rev. C* **87**, 044307 (2013).
 - [4] M. Freer, H. Horiuchi, Y. Kanada-En'yo, D. Lee, and U.-G. Meißner, *Rev. Mod. Phys.* **90**, 035004 (2018).
 - [5] S. Typel, *Phys. Rev. C* **89**, 064321 (2014).
 - [6] W. von Oertzen, *Lect. Notes Phys.* **818**, 109 (2010), arXiv:1004.4247 [nucl-ex].
 - [7] L. M. Satarov, M. I. Gorenstein, A. Motornenko, V. Vovchenko, I. N. Mishustin, and H. Stoecker, *J. Phys. G* **44**, 125102 (2017).
 - [8] L. M. Satarov, R. Poberezhnyuk, I. N. Mishustin, and H. Stoecker, *Phys. Rev. C* **103**, 024301 (2021).
 - [9] S. Misiu, I. N. Mishustin, and W. Greiner, *Mod. Phys. Lett. A* **32**, 1750010 (2016).
 - [10] L. M. Satarov, I. N. Mishustin, A. Motornenko, V. Vovchenko, M. I. Gorenstein, and H. Stoecker, *Phys. Rev. C* **99**, 024909 (2019).
 - [11] L. M. Satarov, M. I. Gorenstein, I. N. Mishustin, and H. Stoecker, *Phys. Rev. C* **101**, 024913 (2020).
 - [12] G. Rosen, *J. Math. Phys. (N.Y.)* **9**, 996, 999 (1968).
 - [13] R. Friedberg, T. D. Lee, and A. Sirlin, *Phys. Rev. D* **13**, 2739 (1976).
 - [14] S. Coleman, *Nucl. Phys. B* **262**, 263 (1985); **269**, 744E (1986).
 - [15] K. Lee, J. A. Stein-Schabes, R. Watkins, and L. M. Widrow, *Phys. Rev. D* **39**, 1665 (1989).
 - [16] S. Misiu and I. N. Mishustin, in *Walter Greiner Memorial Volume*, eds. O. Hess, H. Stöcker, (World Scientific, Singapore, 2017), p. 263; arXiv: 1806.01886 [nucl-th].

- [17] E. P. Gross, *Nuovo Cim.* **20**, 454 (1961).
- [18] L. P. Pitaevskii, *Sov. Phys. JETP* **13**, 451 (1961).
- [19] K. Enquist and M. Laine, *J. Cosmol. Astropart. Phys.* **2003**, 003 (2003); arXiv: cond-mat/0304355.
- [20] E. Nugaev and A. Shkerin, *JETP* **130**, 301 (2020).
- [21] T. D. Lee and Y. Pang, *Phys. Rep.* **221**, 251 (1992).
- [22] A. Kusenko and M. E. Shaposhnikov, *Phys. Lett.* **418**, 46 (1998).
- [23] H. Arodz and J. Lis, *Phys. Rev. D* **79**, 045002 (2009).
- [24] H. Ishihara and A. T. Ogawa, *Phys. Rev. D* **103**, 123029 (2021).
- [25] J. Heeck, A. Rajaraman, and C. B. Verhaaren, *Phys. Rev. D* **104**, 016030 (2021).
- [26] J. W. Clark and T.-P. Wang, *Ann. Phys.* **40**, 127 (1966).
- [27] J.-P. Ebran, E. Khan, T. Niksic, and D. Vretenar, *Phys. Rev. C* **89**, 031303(R) (2014).
- [28] P. Marini *et al.* (INDRA Collaboration), *Phys. Lett. B* **756**, 194 (2016).
- [29] A. A. Zaitsev *et al.*, *Phys. Lett. B* **820**, 136460 (2021).
- [30] A. Yu. Loginov and V. V. Gauzstein, *Phys. Rev. D* **102**, 025010 (2020).
- [31] J. Heeck, A. Rajaraman, R. Riley, and C. B. Verhaaren, *Phys. Rev. D* **103**, 116004 (2021).
- [32] I. N. Mishustin, D. V. Anchishkin, L. M. Satarov, O. S. Stashko, and H. Stoecker, *Phys. Rev. C* **100**, 022201 (2019).
- [33] W. von Oertzen, *Eur. Phys. J. A* **29**, 133 (2006).
- [34] M. Bender, K. Rutz, P.-G. Reinhardt, J. A. Maruhn, and W. Greiner, *Phys. Rev. C* **60**, 034304 (1999).
- [35] C. F. v. Weizsäcker, *Z. Phys.* **96**, 431 (1935).
- [36] J. J. Krauth *et al.*, *Nature* **589**, 527 (2021).
- [37] G. Gamow, *Z. Phys.* **51**, 204 (1928).
- [38] B. Povh, K. Ruth, Ch. Scholz, and F. Zetsche, *Particles and Nuclei*. (Springer, Berlin, 2015).
- [39] I. E. Gulamov, E. Y. Nugaev, A. G. Panin, and M. N. Smolyakov, *Phys. Rev. D* **92**, 045011 (2015).
- [40] W. T. Vetterling, S. A. Teukolsky, W. H. Press, and B. P. Flannery, *Numerical Recipes. Example Book (FORTRAN)*. (Cambridge Press, New York, 1998).
- [41] B. R. Martin and G. Shaw, *Nuclear and Particle Physics*. (Wiley, New York, 2019).